EurJOC
European Journal of Organic Chemistry

A Journal of
ChemPubSoc Europe

Accepted Article

Title: Structural Investigations on Enantiopure P□OP Ligands: a Higher Performing P□OP Ligand for Rhodium-catalyzed Hydrogenations

Authors: Héctor Fernández-Pérez, Bugga Balakrishna, and Anton Vidal-Ferran

To be cited as: *Eur. J. Org. Chem.* 10.1002/ejoc.201701760

Link to VoR: http://dx.doi.org/10.1002/ejoc.201701760

Supported by
ACES Asian Chemical Editorial Society

WILEY-VCH

10.1002/ejoc.201701760

WILEY-VCH

Structural Investigations on Enantiopure P–OP Ligands: a Higher Performing P–OP Ligand for Rhodium-catalyzed Hydrogenations

Héctor Fernández-Pérez,[a] Bugga Balakrishna,[a] and Anton Vidal-Ferran*[a,b]

Dedication ((optional))

Abstract: A second generation of phosphine-phosphite (P–OP) ligands, which incorporates a more sterically bulky phosphite group than previous P–OP ligand designs, gives very efficient catalysts for the Rh-catalyzed asymmetric hydrogenation of a diverse array of substrates (11 examples, from 93% to 99% *ee*) containing structurally diverse substituents and chelating groups at the C=C double bond. The presence of the sterically bulky (S_a)-3,3'-diphenyl-5,5',6,6',7,7',8,8'-octahydro-[1,1'-binaphthalene]-2,2'-diol-derived phosphite fragment caused significant increases in the enantioselectivity (up to Δ*ee* = 58%) and provided improved results to those obtained with the first generation of P–OP-derived rhodium catalysts (i.e. rhodium complexes incorporating the phosphine-phosphite ligands with the (R_a)- and (S_a)-BINOL-derived phosphite groups; BINOL = [1,1'-binaphthalene]-2,2'-diol). Overall, the optimal ligand **L8** provided very high enantioselectivities for an array of structurally diverse olefins (up to 99% *ee*).

Introduction

As a consequence of their singular electronic and steric properties, phosphine-phosphite (P–OP) ligands have emerged as an efficient class of enantiopure bidentate ligands for several transition metal-mediated enantioselective catalytic transformations.[1] For example, BINAPHOS (**L1,** Figure 1) was one of the first enantiopure P–OP ligands to be reported and provided outstanding catalytic properties in the rhodium-mediated asymmetric hydroformylation of structurally diverse olefins.[2] Furthermore, the rhodium complexes derived from P–OP ligands **L2**–**L7** (Figure 1) show high performance in the asymmetric hydrogenation (AH) of functionalized olefins. Following the seminal work of Ruiz et al., which involved the application of sugar-derived P–OP ligand **L2** in asymmetric hydrogenation,[3] a set of structurally diverse enantiopure P–OP ligands **L3**–**L7** has been developed and applied in asymmetric hydrogenations.[1,4] Our group has developed a modular ligand design together with a ligand tuning process that has allowed us to identify a first generation of efficient P–OP ligands for asymmetric hydrogenation (structures **L6** and **L7** in Figure 1).[5a] The optimal ligand structures incorporated an *anti* phosphino alcohol unit with two stereogenic carbons together with a phosphite fragment derived from enantiopure BINOL ([1,1'-binaphthalene]-2,2'-diol). Of the two possible configurations of the BINOL unit, the (S_a)-BINOL-derived P–OP ligand **L6** gives higher enantioselectivities in the hydrogenation of functionalized olefins than does (R_a)-BINOL-derived ligand **L7**. Interestingly, **L6** mediates the asymmetric hydrogenation of a vast array of structurally diverse olefins, including α-(acyl)amino acrylates, itaconic acid derivatives, α-aryl enamides, and α-substituted enol esters (60 examples, full conversion, up to 99% *ee*).[5]

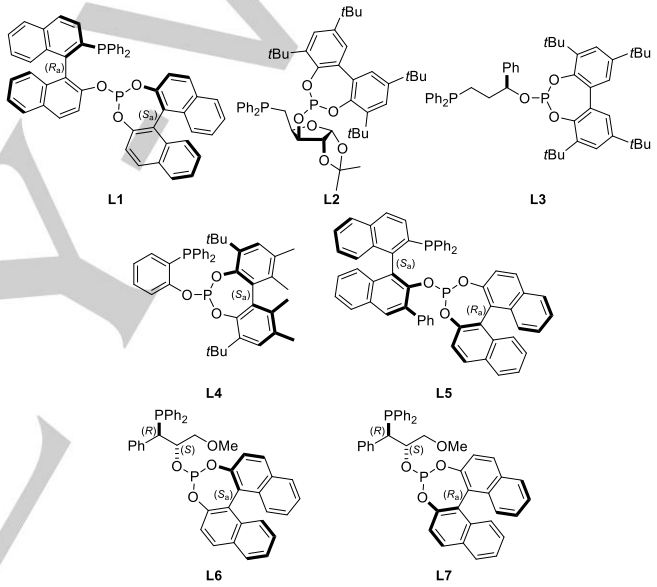

Figure 1. Representative enantiopure P–OP ligands in Rh-mediated AHs.

The wide applicability of **L6** has also been demonstrated by the preparation of advanced synthetic intermediates of active pharmaceutical ingredients (API's) through asymmetric hydrogenation of the appropriate olefin.[6]

The key role of the phosphite fragment of the BINOL-derived P–OP ligand was revealed during DFT studies of the rhodium-catalyzed asymmetric hydrogenation of methyl 2-acetamidoacrylate **S1**.[5b] Firstly, the electronic properties of the phosphite group were found to favor a *cis* relationship between the coordinated olefin (**S1**) and the phosphite group at the square planar rhodium center. That is, the right-hand sides of the quadrant diagrams in Figure 2 are electronically disfavored towards coordination of the olefin carbon atoms. Secondly, the naphthyl rings of the BINOL group, in combination with the phenyl groups of the backbone and phosphine unit, were found to provide steric blocking that prevents placement of the C=C bond in one of the two remaining left-hand quadrants (see Figure 2).

[a] Institute of Chemical Research of Catalonia (ICIQ) and The Barcelona Institute of Science and Technology (BIST), Avgda. Països Catalans 16, 43007 Tarragona, Spain
E-mail: avidal@iciq.cat
https://www.icrea.cat/Web/ScientificStaff/anton-vidal-i-ferran-288
[b] ICREA, Pg. Lluís Companys 23, 08010 Barcelona, Spain

Supporting information for this article is given via a link at the end of the document.((Please delete this text if not appropriate))

Thus, a combination of steric and electronic effects leaves the olefin substrate with only one low-energy direction of approach: towards the lower left quadrant for **L6** and the upper left quadrant for **L7**.[5b] The (*R*)-configuration of the hydrogenation product **P1** obtained with ligand **L6** is predicted by placement of the double bond in the lower left quadrant, coordination of the substrate to the catalyst by the C=O and C=C groups and delivery of dihydrogen across the C=C bond from the metal side (the opposite configuration for product **P1** obtained with ligand **L7** is predicted by placing the substrate in the upper left quadrant, substrate chelation and delivery of dihydrogen from the metal side; see Figure 2). Experimental results have demonstrated that the final configuration of the hydrogenation products derived from α-(acylamino)acrylates, itaconic acid derivatives and their analogues, α-arylenamides, and α-substituted enol esters can always be predicted to be (*R*)-, (*S*)-,[7] (*R*)-, and (*R*), respectively when ligand **L6** is employed.[5d] These configurations are obtained following the stereochemical model indicated above (placement of the double bond in the lower left quadrant, substrate chelation and delivery of dihydrogen from the metal side).

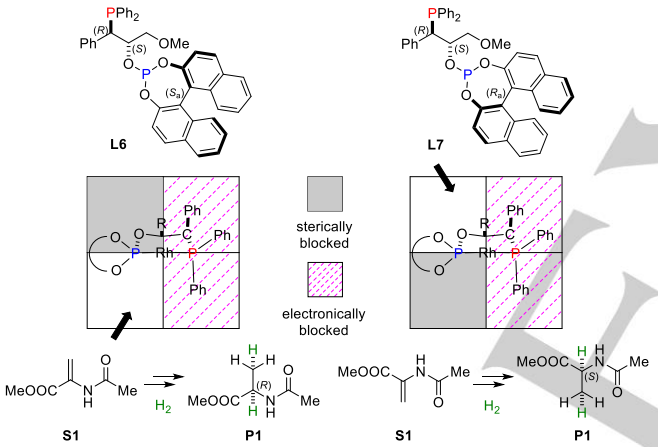

Figure 2. Rationalization of the stereochemical outcome of AHs mediated by rhodium complexes of **L6** and **L7**.

In our quest to develop higher-performing ligands, we have also reduced the distance between the phosphine and phosphite groups by one bond.[8] However, enantioselectivities higher than those afforded by **L6** were not obtained.[8] Our most recent efforts towards higher performing ligands for rhodium mediated asymmetric hydrogenations are based on modifying the structure of the [1,1'-biaryl]-2,2'-diol-derived phosphite group by introducing substituents at the positions more prone to affecting the steric environment around the rhodium center.

Herein, we wish to report the application of ligands **L8** and **L9** in Rh-catalyzed AHs,[9] which incorporate a sterically bulky phosphite fragment derived from 3,3'-diphenyl-5,5',6,6',7,7',8,8'-octahydro-[1,1'-binaphthalene]-2,2'-diol (*o*-Ph-H8-BINOL) (Figure 3). In these ligands, the substituents at the 3 and 3' positions of the [1,1'-biaryl]-2,2'-diol-derived phosphite group have been modified while maintaining the phosphine groups and carbon backbone design of **L6**. Metal complexes derived from these ligands are efficient and highly enantioselective catalysts in the Rh-mediated hydrogenative kinetic resolution of vinyl sulfoxides[9] and the Ir-catalyzed asymmetric hydrogenation of seven-membered C=N-containing heterocyclic compounds.[10] The discussion that follows highlights the preparation and characterization of cationic P–OP-Rh complexes derived from **L8** and **L9** and their use as pre-catalysts in the asymmetric hydrogenation of an array of structurally diverse functionalized olefins.

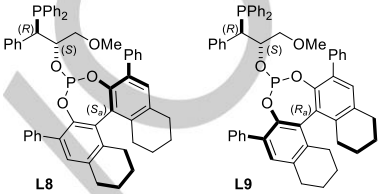

Figure 3. Second generation of enantiopure P–OP ligands **L8** and **L9**.

Results and Discussion

We initially investigated the preparation of [Rh(nbd)(**L8**)]BF_4 (**C1**) and [Rh(nbd)(**L9**)]BF_4 (**C2**) in order to study the effectiveness of these complexes in asymmetric hydrogenation reactions. Pre-catalyst **C1** has been previously prepared by our group in a two-step gram-scale and chromatography-free procedure.[11] Complex **C2** was prepared in high yield by reacting stoichiometric amounts of P–OP ligand **L9** with $[Rh(nbd)_2]BF_4$ in DCM (Scheme 1), and was fully characterized by standard techniques.

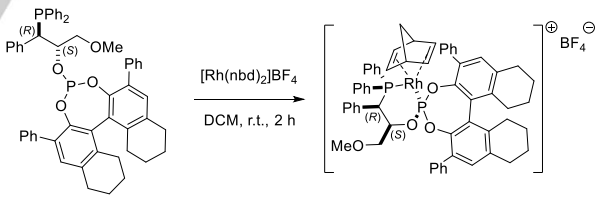

L8 (S_a)-*o*-Ph-H8-BINOL
L9 (R_a)-*o*-Ph-H8-BINOL
C1 (S_a)-*o*-Ph-H8-BINOL (87% yield)
C2 (R_a)-*o*-Ph-H8-BINOL (86% yield)

Scheme 1. Preparation of rhodium pre-catalysts **C1** and **C2** derived from P–OP ligands **L8** and **L9**, respectively.

In order to gain information about the structural features of coordinated P–OP ligands **L8** and **L9**, single crystals of complexes **C1** and **C2** were analyzed by X-ray crystallography. ORTEP views of the molecular structures of these rhodium complexes, along with selected bond lengths and angles, are shown in Figure 4 and Figure 5. Both complexes display square-planar coordination geometry and both ligands coordinate with similar bite angles (91.80(5)º and 91.97(3)º for complexes **C1** and **C2**, respectively). The Rh-P distance is shorter for the phosphite group than for the phosphine group.

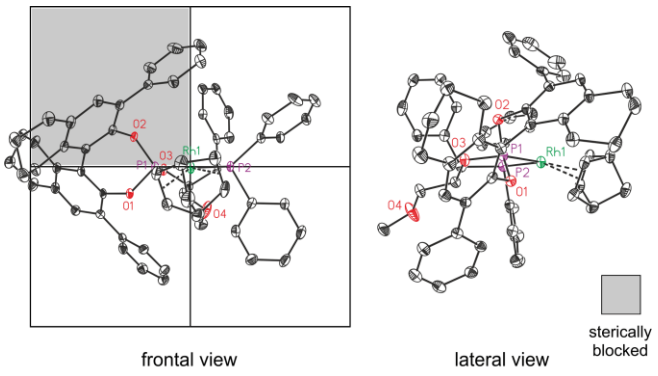

Complex **C1**

Figure 4. Crystal structure of the Rh-complex **C1** (frontal and lateral ORTEP drawings showing thermal ellipsoids at 30% probability). The H-atoms and BF_4^- counterion have been omitted for clarity. Selected bond lengths [Å] and angles [º]: Rh1-P1 = 2.1975(14), Rh1-P2 = 2.3286(14), P1-Rh1-P2 = 91.80(5).

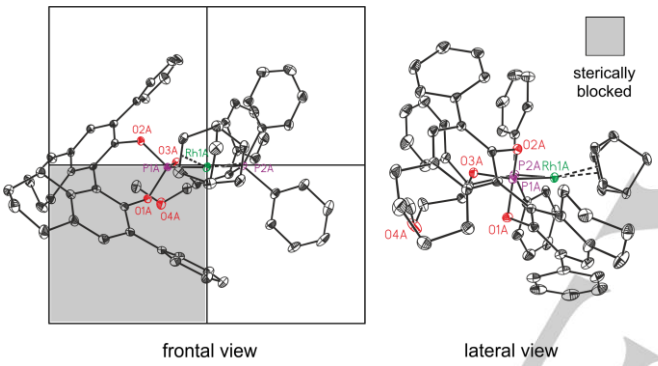

Complex **C2**

Figure 5. Crystal structure of the Rh-complex **C2** (frontal and lateral ORTEP drawings showing thermal ellipsoids at 30% probability). The H-atoms and BF_4^- counterion have been omitted for clarity. Selected bond lengths [Å] and angles [º]: Rh1A-P1A = 2.2014(7), Rh1A-P2A = 2.3214(9), P1A-Rh1A-P2A = 91.97(3).

Analysis of the three-dimensional arrangement of the ligand in complex **C1** indicates that the P-Rh-P coordination plane roughly bisects the phosphite fragment (see frontal view for complex **C1** in Figure 4). As can also be seen from this view, **L8** has a similar orientation to **L6.** Furthermore, one of the phenyl groups in the *ortho*-position is located above the P-Rh-P coordination plane and is mostly confined to the upper left quadrant. Ligand **L9** takes on a similar three-dimensional arrangement in complex **C2** as ligand **L8** does in complex **C1**; however, the phenyl group in the *ortho*-position is now located below the P-Rh-P coordination plane and is mostly confined to the lower left quadrant (Figure 5). Overall, the occupation of the upper left and lower left quadrants in rhodium complexes derived from ligands **L8** and **L9**, respectively, appears to be greater than for those of the analogous ligands lacking phenyl substituents at the 3 and 3' positions of the [1,1'-biaryl]-2,2'-diol.[12] Supported by the computational studies discussed above,[5b] we hypothesized that the rhodium complexes derived from our second generation of ligands **L8** and **L9** might provide higher enantioselectivities than those obtained with their 3,3'-unsubstituted analogues **L6** and **L7**.

Table 1. AH of functionalized model substrates **S2**–**S5** catalyzed by rhodium complexes derived from P–OP ligands **L6**–**L10**[a]

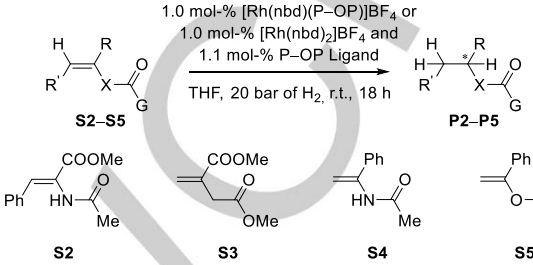

Entry	Lig.	Subs. **S2**[b]	Subs. **S3**[b]	Subs. **S4**[b]	Subs. **S5**[b]
1[c]	**L6**	99% *ee* (*R*)	99% *ee* (*S*)	98% *ee* (*R*)	96% *ee* (*R*)
2	**L7**	86% *ee* (*S*)[c]	97% *ee* (*R*)	94% *ee* (*S*)	90% *ee* (*S*)
3	**L8**	**99% *ee* (*R*)**	**99% *ee* (*S*)**	**99% *ee* (*R*)**	**99% *ee* (*R*)**[d]
4	**L9**	96% *ee* (*S*)	99% *ee* (*R*)	98% *ee* (*S*)	99% *ee* (*S*)
5	**L10**	93% *ee* (*S*)	92% *ee* (*R*)	88% *ee* (*S*)	94% *ee* (*S*)

[a] The values shown are the average of at least of two independent runs. Conversions determined by ^{1}H NMR and > 99% unless indicated. [b] Enantiomeric excesses were determined by HPLC or GC analysis on chiral stationary phases. Absolute configurations were assigned by comparison of chromatographic elution orders with reported data. [c] Results published in references 5b and 5d. [d] 96% conversion.

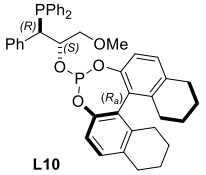

Catalytic studies to test this hypothesis were performed under standard catalyst screening conditions (1.0 mol-% of pre-formed or in situ prepared [Rh(nbd)(P–OP)] complex as the catalyst precursor, 20 bar of H_2, THF as solvent, room temperature, and 18 h reaction time).[5d,8] A structurally diverse array of model substrates was tested: α-(acyl)amino acrylate **S2**, itaconic acid derivative **S3**, α-aryl enamide **S4**, and α-substituted enol ester **S5**. The results of this comparative study are summarized in entries Table 1, and hydrogenation results from rhodium pre-catalysts bearing the previously reported first generation of ligands (i.e., **L6** and **L7**)[5b,d] are included to aid comparison (entries 1 to 4 in Table 1).

All the rhodium complexes performed very efficiently in terms of activity, with complete conversion towards the hydrogenated products **P2**–**P5** obtained in almost all cases. However, as far as enantioselectivity is concerned, the presence of the *o*-Ph-H8-BINOL unit in ligands **L8** and **L9** led to an

enhancement in the enantioselectivity for all substrates compared with the results for complexes bearing 3,3'-unsubstituted ligands **L6** and **L7** (compare entries 1 with 3 and entries 2 with 4 in Table 1, respectively). An increase of up to 9% *ee* was reached in the hydrogenation of substrate **S5** using the rhodium complex derived from ligand **L9** (compare entry 2 with entry 4 for substrate **S5** in Table 1).

To prove that the enhanced enantioselectivities obtained with the second generation of P–OP ligands were mainly due to the introduction of substituents at the 3 and 3' positions of the [1,1'-biaryl]-2,2'-diol-derived phosphite, and not due to the replacement of the binaphthyl group by the 5,5',6,6',7,7',8,8'-octahydro-binaphthyl motif,[12] we assessed the catalytic performance of ligand **L10**[13] in the hydrogenation of substrates **S2**–**S5** (Table 1). Interestingly, slightly lower *ee*'s were observed for substrates **S3** and **S4** with ligand **L10** than with ligand **L7**, whilst an opposite trend was observed for **S2** and **S5** (compare entry 2 with entry 5, Table 1). It is also interesting to note that the *ee*'s obtained with **L10** for the four model substrates did not surpass those with **L9** (compare entry 4 with entry 5, Table 1), which proves that the introduction of substituents at the 3 and 3' positions of the [1,1'-biaryl]-2,2'-diol-derived phosphite plays a major role in the enhancement of the *ee*'s in substrates **S2**–**S5**.

It is noteworthy that the rhodium complex bearing ligand **L8** gave perfect enantioselectivities (99% *ee*) for the four model substrates (entry 3, Table 1), and is the highest-performing P–OP ligand developed by our research group for the Rh-mediated asymmetric hydrogenation of functionalized olefins. Encouraged by our results, we decided to assess the performance of **L8** in the asymmetric hydrogenation of a broader set of structurally diverse functionalized olefins, of which some underwent hydrogenation with unsatisfactory enantioselectivities when ligand **L6** was employed.[5]

A set of α-(acyl)amino acrylates **S6**–**S8** was hydrogenated with excellent enantioselectivities regardless of the substitution pattern at the aromatic ring (entries 1–3, Table 2). It should be noted that the challenging cyclic enamide **S9** was hydrogenated with full conversion and excellent enantioselectivity (96% *ee*) in favor of the (*R*)-configured product (entry 4, Table 2). The enantioselectivity that we have obtained under mild hydrogenation conditions is very close to the highest reported one for enantiopure rhodium(I) catalyst derived from chiral bidentate phosphorus ligands (98% *ee* for the rhodium catalyst derived from Me-PennPhos,[14a] and 96% *ee* for the rhodium catalyst derived from Phthalaphos[14b]).

Following the same trend, the enantioselective hydrogenation of sterically encumbered *N*-(1-(naphthalen-1-yl)vinyl)acetamide **S10** provided the hydrogenated product with complete conversion and a 93% *ee* (entry 5, Table 2). These results compete with those of the highest-performing rhodium catalysts reported in the literature (93% *ee* for the rhodium catalyst derived from a phosphine–phosphoramidite ligand,[15a] and 97% *ee* for the rhodium catalyst derived from DioxyBenzP*[15b]). It is interesting to note that the hydrogenation product of **S10** is an advanced intermediate in the synthesis of cinacalcet hydrochloride, which is used for the treatment of secondary hyperparathyroidism.[16]

The 5-fluoropyridin-2-yl-substituted vinyl acetamide **S11** was also subjected to hydrogenation using the rhodium catalyst derived from **L8**. High enantioselectivity (98% *ee*, see entry 6 in Table 2) was observed, but only moderate conversion was obtained. The resulting hydrogenated product is a valuable precursor to chiral drugs that are currently in clinical development for cancer therapy.[17]

Table 2. AH of functionalized olefins using [Rh(nbd)(**L8**)]BF_4 as catalyst.[a]

Entry	Substrate	p (H_2, bar)	Conv. [%][b]	*ee* [%][c]
1	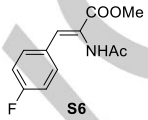 **S6**	20	> 99	99 (*R*)
2	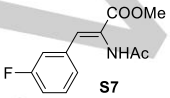 **S7**	20	> 99	99 (*R*)
3	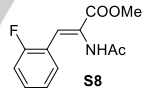 **S8**	20	> 99	99 (*R*)
4	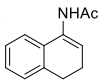 **S9**	20	> 99	96 (*R*)
5	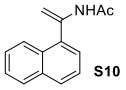 **S10**	40	> 99	93 (*R*)
6[d]	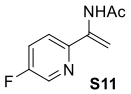 **S11**	80	42 (39)[e]	98 (*R*)
7	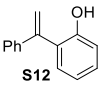 **S12**	20	> 99	99 (*R*)

[a] The values shown are the average of at least of two independent runs. Hydrogenations were run in a parallel reactor: Reaction conditions: [Rh(nbd)(**L8**)]BF_4/substrate=1.0:100, r.t., substrate concentration=0.20 M in THF, 18 h. [b] Conversions determined by ^{1}H NMR. Typical isolated yields were >90%. [c] Enantiomeric excesses were determined by HPLC analysis on chiral stationary phases. Absolute configurations were assigned by comparison of chromatographic elution orders with reported data. [d] [Rh(nbd)(**L8**)]BF_4/substrate=2.0:100. [e] Isolated yield in parenthesis.

Further interesting substrates for asymmetric hydrogenation contain an aromatic hydroxyl group that coordinates to rhodium and assists the hydrogenation reaction. Substrate **S12** was examined as a model substrate for this type of olefin.[18] Perfect enantioselectivity was obtained with ligand **L8**, and the

hydrogenated product was obtained with full conversion (99% *ee*, entry 7, Table 2).

The results highlighted in Table 3 provide a comparison of the results obtained for catalysts containing **L6** or **L8** in the hydrogenation of a set of structurally diverse substrates. In all cases the enantioselectivities obtained for the new ligand with substituents at the 3 and 3' positions of the (S_a)-[1,1'-biaryl]- 2,2'-diol-derived phosphite group were either equally high or superior. Significant enhancements in the enantioselectivity were obtained (up to 58% for substrate **S12**, see entry 9 in Table 3), even for challenging substrates such as **S9** and **S10** for which many reported ligands fail to provide high enantioselectivities (see entries 6 and 7 in Table 3).[15a,19] The results highlighted in Table 3 also illustrate that the configuration of the hydrogenated product can be predicted for all substrates: the substrate is placed in the lower left quadrant, simultaneous coordination of the C=C bond and the substrate's chelating group to the rhodium center occurs, then delivery of dihydrogen across the C=C double bond from the side of the metal gives the hydrogenated product. It should be noted that the change to the (*S*)-configuration in the hydrogenation products of itaconic acid derivative **S3** is due to an inversion in the CIP priority rules and not to a breach of the previous rule.

Table 3. Comparative table on AHs of a set of functionalized substrates using rhodium complexes derived from P–OP ligands **L6** and **L8**.

Entry	Substrate	Ligand **L6**	Ligand **L8**	Δ*ee* [%]
1	**S2**	Conv. > 99% 99% *ee* (*R*)	Conv. > 99% 99% *ee* (*R*)	=
2	**S3**	Conv. > 99% 99% *ee* (*S*)	Conv. > 99% 99% *ee* (*S*)	=
3	**S4**	Conv. > 99% 98% *ee* (*R*)	Conv. > 99% 99% *ee* (*R*)	**+1**
4	**S5**	Conv. > 99% 96% *ee* (*R*)	Conv. = 96% 99% *ee* (*R*)	**+3**
5	**S6**	Conv. > 99% 99% *ee* (*R*)	Conv. > 99% 99% *ee* (*R*)	=
6	**S9**	Conv. > 99% 57% *ee* (*R*)	Conv. > 99% 96% *ee* (*R*)	**+39**
7	**S10**	Conv. = 90% 83% *ee* (*R*)	Conv. > 99% 93% *ee* (*R*)	**+10**
8	**S11**	Conv. = 50% 98% *ee* (*R*)	Conv. = 42% 98% *ee* (*R*)	=
9	**S12**	Conv. = 57% 41% *ee* (*R*)	Conv. > 99% 99% *ee* (*R*)	**+58**

A computational study on the relative energies of the transition states of the rate- and stereo-determining step—oxidative addition of dihydrogen to the ligand-substrate rhodium complexes[5b] —for all substrates and at a sufficiently high computational level would certainly allow the experimental results obtained for ligands **L8** and **L9** to be rationalized. Unfortunately, it is not feasible to carry out such a study due to the enormous computational capacity required. However, computational studies on the asymmetric hydrogenation of the simplest possible olefin (methyl 2-acetamidoacrylate, **S1**) using the rhodium complexes derived from BINOL-derived P–OP ligand **L6**[5b] paved the way for the rationalization of the results presented herein. The accepted view for the steric requirements of these substrates is that, in the transition state, the steric hindrance appears in the quadrant originally occupied by the olefin carbon substituted with the chelating group (C_α).[20] There-

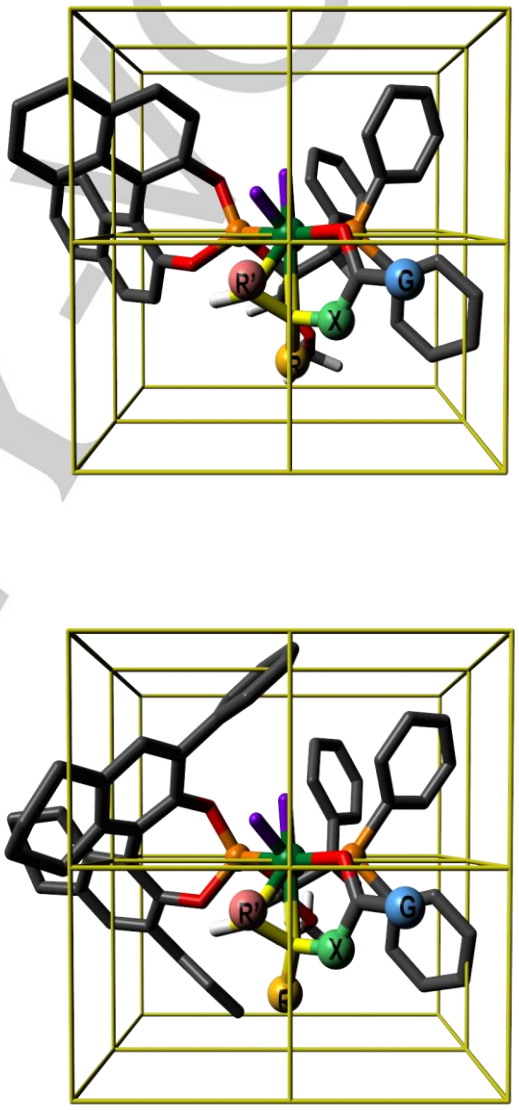

Figure 6. Three dimensional representation of the oxidative addition transition states (OATS) for the most favored reaction manifold in the AH of a general olefin catalyzed by Rh-complexes derived from P–OP ligand **L6** (top) or **L8** (bottom). The OATS structure for **L6** (top) was already described in ref. [5b]. The depicted OATS structure for **L8** (bottom) is the result of the replacement of ligand **L6** for **L8** and it does not correspond to an optimized structure.

fore, preferential placement of C_α in the lower-left quadrant of the two-dimensional representation shown in Figure 2 (or in the front-lower-left octant in the three-dimensional representation in Figure 6), places the substrate far from the steric congestion of the binaphthyl group. This translates into improved enantioselectivities when the ligands incorporate a (S_a)-configured [1,1'-biaryl]-2,2'-diol-derived phosphite group. Assuming that the stereoelectronic effects operating in the asymmetric hydrogenations involving ligand **L6** also apply to those of **L8** (cfr. to the introduction of this manuscript), increasing the occupancy of the front-upper-left octant, for instance by introducing substituents at 3 and 3' positions of the (S_a)-[1,1'-biaryl]-2,2'-diol-derived phosphite group, should translate into higher enantioselectivities of the hydrogenation products. As discussed above, this working hypothesis was indeed demonstrated at the experimental level: in all cases, enantioselectivities obtained with **L8** equaled or surpassed those obtained with **L6**. We are aware that predicting changes to the enantioselectivity of this complex transformation cannot be justified solely in terms of the substitution pattern of the [1,1'-biaryl]-2,2'-diol-derived phosphite group: manifolds involving placement of the C=C bond in the right-handed octants may also be intervening at a low extent.[5b] However, we expect that the work presented herein demonstrates that analysis based on octant diagrams for a mechanistically well-understood reaction may prove useful in designing improved ligands. This strategy is currently being applied to the design and development of new ligands having better performance in transformations of interest, such as hydroformylation. The results will be reported in due course.

Conclusions

The preparation of rhodium pre-catalysts derived from P–OP ligands incorporating the sterically bulky *o*-Ph-H8-BINOL-derived phosphite is reported. Structural investigations into the coordination features of the new P–OP ligands in rhodium pre-catalysts for asymmetric hydrogenations have provided insight into the origin of the increased enantioselectivities obtained for the asymmetric hydrogenations involving these ligands compared with those for reported P–OP ligands lacking substituents at the 3 and 3' positions of the [1,1'-biaryl]-2,2'-diol-derived phosphite group. Of the two described ligands, ligand **L8**, which incorporates the sterically bulky (S_a)-*o*-Ph-H8-BINOL-derived phosphite fragment, provided perfect enantioselectivities for an array of eleven structurally diverse olefins (*ee*'s ranging from 93 to 99% *ee*, mean *ee* value of 98% with an standard deviation of 1.8 % *ee*).

Experimental Section

General considerations: All syntheses were carried out using chemicals as purchased from commercial sources, unless otherwise stated. Glassware was dried under vacuum and heated with a hot air gun before use. All manipulations and reactions were run under inert atmosphere using anhydrous solvents, in either a glove box or with standard Schlenk-type techniques. All solvents were dried by using a Solvent Purification System (SPS). Silica gel 60 (230–400 mesh) was used for column chromatography. NMR spectra were recorded in $CDCl_3$ unless otherwise noted, using a 400 MHz or 500 MHz spectrometer. ^1H and $^{13}C\{^1H\}$ NMR chemical shifts are quoted in ppm relative to residual solvent peaks, whereas $^{31}P\{^1H\}$ chemical shifts are quoted in ppm relative to 85% phosphoric acid in water. $^{19}F\{^1H\}$ NMR chemical shifts are quoted in ppm relative to $BF_3{\cdot}OEt_2$ in $CDCl_3$. High resolution mass spectra (HRMS) were recorded by using an ESI ionization method in positive mode. Optical rotations were measured on a Jasco P-1030 polarimeter. Melting points were measured in open capillaries on a Büchi B-540 instrument and are uncorrected. Enantiomeric excesses were determined by GC or HPLC on using chiral stationary phases. GC analyses were performed on an Agilent 6890N chromatograph equipped with a FID detector. HPLC analyses were performed on an Agilent 1200 Series chromatograph equipped with a diode array UV detector.

General synthetic procedure for the preparation of Rh-pre-catalyst: A solution of the P–OP ligand (1.0 mmol) in anhydrous dichloromethane (5.0 mL) was slowly added *via* cannula to a stirred solution of $[Rh(nbd)_2]BF_4$ (0.98 mmol) in anhydrous dichloromethane (5.0 mL). The reaction was stirred for 2 h at room temperature under argon atmosphere, after which the dichloromethane solvent was evaporated off until the mixture had one fourth of its original volume. Anhydrous diethyl ether (15.0 mL) was slowly added by syringe and the resulting solution was slowly stirred to yield an orange suspension. The precipitate was filtered off under inert atmosphere by using a cannula filter and the resulting solid was washed with anhydrous diethyl ether (2 x 12.0 mL) and dried *in vacuo* to afford the pure $[Rh(nbd)(P–OP)]BF_4$ complex as an orange powder.

$[Rh(nbd)(L8)]BF_4$ complex (C1): Rhodium complex **C1** was prepared by following the general procedure, starting from P–OP ligand **L8** (0.088 g, 0.106 mmol) and $[Rh(nbd)_2]BF_4$ (0.039 g, 0.101 mmol). It was obtained as an orange powder (0.097 g, 87% isolated yield). The characterization data of complex **C1** has already been published.[11]

$[Rh(nbd)(L9)]BF_4$ complex (C2): Rhodium complex **C2** was prepared by following the general procedure, starting from P–OP ligand **L9** (0.197 g, 0.239 mmol) and $[Rh(nbd)_2]BF_4$ (0.088 g, 0.234 mmol). It was obtained as an orange powder (0.227 g, 86% isolated yield). ^1H NMR (400 MHz, CD_2Cl_2) δ 7.84–7.74 (m, 2H), 7.62–7.39 (m, 9H), 7.37–7.14 (m, 5H), 7.10–6.85 (m, 7H), 6.76–6.71 (m, 2H), 6.35–6.24 (m, 2H), 5.93 (bs, 1H), 5.16 (bs, 1H), 4.52–4.44 (m, 1H), 4.02–3.96 (m, 2H), 3.86 (bs, 1H), 3.61 (bd, J = 14.5 Hz, 1H), 3.13–2.60 (m, 11H), 2.49–2.26 (m, 2H), 1.96–1.54 (m, 10H); $^{13}C\{^1H\}$ NMR (100 MHz, CD_2Cl_2) δ 143.4 (C), 143.3 (C), 142.5 (C), 142.4 (C), 139.8 (C), 138.3 (C), 137.9 (C), 137.5 (C), 137.1 (C), 136.7 (C), 135.3 (CH), 135.2 (CH), 132.70 (C), 132.68 (C), 132.4 (C), 132.3 (C), 132.09 (C), 132.07 (C), 131.9 (CH), 131.82 (CH), 131.82 (CH), 131.79 (CH), 131.69 (CH) 131.62 (CH), 131.59 (CH), 131.4 (CH), 130.74 (CH), 130.70 (CH), 130.4 (CH), 130.3 (CH), 129.9 (C), 129.8 (CH), 129.7 (CH), 129.5 (C), 129.4 (C), 129.3 (C), 129.2 (C), 129.1 (CH), 129.0 (CH), 128.94 (CH), 128.88 (CH), 128.77 (CH), 128.3 (CH), 128.2 (C), 128.1 (C), 127.64 (CH), 127.62 (CH), 103.3–102.9 (m, CH), 99.9–99.6 (m, CH), 93.0–92.8 (m, CH), 78.6 ($^2J_{C\text{-}P}$ = 8.1 Hz, CH), 75.5 (CH), 72.8 (CH_2), 71.7 (CH_2), 59.6 (CH_3), 56.3 (CH), 55.3 (CH), 43.7 (d, $^1J_{C\text{-}P}$ = 24.6 Hz, CH), 29.8 (CH_2), 29.7 (CH_2), 28.4 (CH_2), 28.3 (CH_2), 23.13 (CH_2), 23.1 (CH_2), 23.0 (CH_2); $^{31}P\{^1H\}$ NMR (162 MHz, CD_2Cl_2) δ 131.3 (dd, $^1J_{Rh\text{-}P}$ = 265.2 Hz, $^2J_{P\text{-}P}$ = 68.9 Hz, P–O), 27.7 (dd, $^1J_{Rh\text{-}P}$ = 146.8 Hz, $^2J_{P\text{-}P}$ = 68.9 Hz, P–C). HRMS (ESI^+) [Calculated for $C_{61}H_{58}O_4P_2Rh$ $(M–BF_4)^+$ 1019.2860; observed 1019.2833].

General procedure for the Rh-mediated asymmetric hydrogenation of functionalized substrates: A solution of the required amount of $[Rh(nbd)_2]BF_4$ (1.0 mol-%) and P–OP ligand **L8**– **L9** (1.1 mol-%) and the corresponding functionalized olefin (0.10 mmol) in anhydrous and degassed tetrahydrofuran (0.50 mL) was prepared inside a glass vessel under N_2 atmosphere working in a glove box. In all cases, the molar concentration of a given substrate in the reaction medium was adjusted to 0.20 M. Once the reaction mixture had been loaded, the glass vessel was then placed into one of the positions of a steel autoclave reactor (HEL Cat-24 parallel pressure multireactor). The autoclave was purged three times with H_2 gas (at a pressure not higher than the selected one) and finally, the autoclave was pressurized under the required pressure of H_2 gas. The reaction mixture was stirred at r.t. for 18 h (overnight reaction). The autoclave was then slowly depressurized. The reaction mixture was filtered through a short pad of SiO_2 and eluted with ethyl acetate (1.0 mL). The resulting solution was concentrated under vacuum and the conversion was determined by ^1H NMR. The enantiomeric excess was determined by GC or HPLC analysis on chiral stationary phases.

Supporting Information (see footnote on the first page of this article): X-ray crystal structures (CCDC 1589126-1589127), ^1H, ^{13}C, and ^{31}P NMR spectra of all new compounds, chiral GC and HPLC analyses of the catalytic reactions.

Acknowledgements

We thank MINECO (CTQ2014-60256-P and Severo Ochoa Excellence Accreditation SEV-2013-0319), the ICIQ Foundation for financial support, and Dr. J. Benet-Buchholz for X-ray crystallographic analysis. B. Balakrishna thanks the AGAUR for a pre-doctoral fellowship (2013FI-B 00545). We are grateful to Rosie Somerville for proofreading the manuscript.

Keywords: Asymmetric catalysis • Hydrogenation • Rhodium • Bidentate ligands • P ligands

[1] For general reviews, see: a) H. Fernández-Pérez, P. Etayo, A. Panossian, A. Vidal-Ferran, *Chem. Rev.* **2011**, *111*, 2119-2176; b) J. Wassenaar, J. N. H. Reek, *Org. Biomol. Chem.* **2011**, *9*, 1704-1713; c) A. Pizzano, *Chem. Rec.* **2016**, *16*, 2595-2618.

[2] a) N. Sakai, S. Mano, K. Nozaki, H. Takaya, *J. Am. Chem. Soc.* **1993**, *115*, 7033-7034; b) K. Nozaki, H. Takaya, T. Hiyama, *Top. Catal.* **1997**, *4*, 175-185.

[3] O. Pàmies, M. Diéguez, G. Net, A. Ruiz, C. Claver, *Chem. Commun.* **2000**, 2383-2384.

[4] For ligand **L3**, see the reference: a) S. Deerenberg, O. Pàmies, M. Diéguez, C. Claver, P. C. J. Kamer, P. W. N. M. van Leeuwen, *J. Org. Chem.* **2001**, *66*, 7626-7631; for ligand **L4**, see the reference: b) A. Suárez, A. Pizzano, *Tetrahedron: Asymmetry* **2001**, *12*, 2501-2504; for ligand **L5**, see the reference: c) Y. Yan, Y. Chi, X. Zhang, *Tetrahedron: Asymmetry* **2004**, *15*, 2173-2175.

[5] a) H. Fernández-Pérez, M. A. Pericàs, A. Vidal-Ferran, *Adv. Synth. Catal.* **2008**, *350*, 1984-1990; b) H. Fernández-Pérez, S. M. A. Donald, I. J. Munslow, J. Benet-Buchholz, F. Maseras, A. Vidal-Ferran, *Chem. Eur. J.* **2010**, *16*, 6495-6508; c) H. Fernández-Pérez, P. Etayo, J. L. Núñez-Rico, A. Vidal-Ferran, *Chim. Oggi* **2010**, *28*, XXVI-XXVIII; d) J. L. Núñez-Rico, P. Etayo, H. Fernández-Pérez, A. Vidal-Ferran, *Adv. Synth. Catal.* **2012**, *354*, 3025-3035.

[6] P. Etayo, J. L. Núñez-Rico, H. Fernández-Pérez, A. Vidal-Ferran, *Chem. Eur. J.* **2011**, *17*, 13978-13982.

[7] The change to the (*S*)-configuration in the hydrogenation products of itaconic acid derivatives and analogues is due to an inversion in the CIP priority rules.

[8] a) H. Fernandez-Perez, J. Benet-Buchholz, A. Vidal-Ferran, *Org. Lett.* **2013**, *15*, 3634-3637; b) H. Fernandez-Perez, J. Benet-Buchholz, A. Vidal-Ferran, *Chem. Eur. J.* **2014**, *20*, 15375-15384; c) J. R. Lao, J. Benet-Buchholz, A. Vidal-Ferran, *Organometallics* **2014**, *33*, 2960-2963.

[9] For the synthesis and characterization data of ligands **L8** and **L9**, see: J. R. Lao, H. Fernández-Pérez, A. Vidal-Ferran, *Org. Lett.* **2015**, *17*, 4114-4117.

[10] B. Balakrishna, A. Bauzá, A. Frontera, A. Vidal-Ferran, *Chem. Eur. J.* **2016**, *22*, 10607-10613.

[11] For the experimental preparation and characterization data, see the following reference: B. Balakrishna, A. Vidal-Ferran, *Synthesis* **2016**, *48*, 997-1001.

[12] Partially hydrogenated binaphthyl motifs in ligands **L8** and **L9** present larger dihedral angles between the two aryl rings than those containing naphthyl fragments. This geometrical parameter usually translates into higher occupation volumes. For a general review on this topic, see the following reference: T. T.-L. Au-Yeng, S.-S. Chan, A. S. C. Chan, *Adv. Synth. Catal.* **2003**, *345*, 537-555.

[13] The synthesis and characterization data of ligand **L10** have been reported in the reference [10].

[14] Using a rhodium catalyst derived from Me-PennPhos ligand, see: a) Z. Zhang, G. Zhu, Q. Jiang, D. Xiao, X. Zhang, *J. Org. Chem.* **1999**, *64*, 1774-1775; or using a rhodium catalyst derived from Phthalaphos ligand, see: b) L. Pignataro, M. Boghi, M. Civera, S. Carboni, U. Piarulli, C. Gennari, *Chem. Eur. J.* **2012**, *18*, 1383-1400.

[15] Using a rhodium catalyst derived from triphosphorous bidentate phosphine–phosphoramidite ligand, see: a) W. Zhang, X. Zhang, *Angew. Chem., Int. Ed.* **2006**, *45*, 5515-5518; or using a rhodium catalyst derived from DioxyBenzP* ligand, see: b) T. Imamoto, K. Tamura, Z. Zhang, Y. Horiuchi, M. Sugiya, K. Yoshida, A. Yanagisawa, I. D. Gridnev, *J. Am. Chem. Soc.* **2012**, *134*, 1754-1769.

[16] G. B. Shinde, N. C. Niphade, S. P. Deshmukh, R. B. Toche, V. T. Mathad, *Org. Process Res. Dev.* **2011**, *15*, 455-461, and references cited therein for recent synthetic approaches towards cinacalcet.

[17] a) T. Wang, S. Ioannidis, L. Almeida, M. H. Block, A. M. Davies, M. L. Lamb, D. A. Scott, M. Su, H.-J. Zhang, M. Alimzhanov, G. Bebernitz, K. Bell, M. Zinda, *Bioorg. Med. Chem. Lett.* **2011**, *21*, 2958-2961; b) S. Ioannidis, M. L. Lamb, T. Wang, L. Almeida, M. H. Block, A. M. Davies, B. Peng, M. Su, H.-J. Zhang, E. Hoffmann, C. Rivard, I. Green, T. Howard, H. Pollard, J. Read, M. Alimzhanov, G. Bebernitz, K. Bell, M.-W. Ye, D. Huszar, M. Zinda, *J. Med. Chem.* **2011**, *54*, 262-276; c) M. B. Sonbol, B. Firwana, A. Zarzour, M. Morad, V. Rana, R. V. Tiu, *Ther. Adv. Hematol.* **2013**, *4*, 15-35.

[18] X. Wang, A. Guram, S. Caille, J. Hu, J. P. Preston, M. Ronk, S. Walker, *Org. Lett.* **2011**, *13*, 1881-1883.

[19] a) M. J. Burk, G. Casy, N. B. Johnson, *J. Org. Chem.* **1998**, *63*, 6084−6085; b) B. Mohar, M. Stephan, *Adv. Synth. Catal.* **2013**, *355*, 594-600.

[20] For example, see: C. R. Landis, S. Feldgus, *Angew. Chem., Int. Ed.* **2000**, *39*, 2863-2866.

Entry for the Table of Contents (Please choose one layout)

Layout 1:

FULL PAPER

Text for Table of Contents

((Insert TOC Graphic here: max. width: 5.5 cm; max. height: 5.0 cm; NOTE: the final letter height should not be less than 2 mm.))

Key Topic*

*Author(s), Corresponding Author(s)**

Page No. – Page No.

Title

*one or two words that highlight the emphasis of the paper or the field of the study

Layout 2:

FULL PAPER

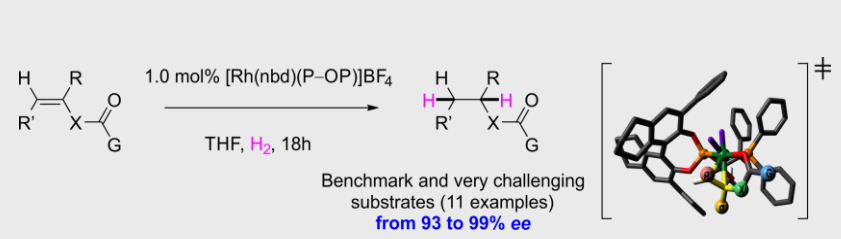

Asymmetric Hydrogenation*

*Héctor Fernández-Pérez, Bugga Balakrishna, Anton Vidal-Ferran**

Page No. – Page No.
Structural Investigations on Enantiopure P–OP Ligands: a Higher Performing P–OP Ligand for Rhodium-catalyzed Hydrogenations

*A second generation of phosphine-phosphite (*a.k.a.* P–OP) ligands, which incorporates a more voluminous phosphite group than in previous P–OP ligand designs, led to very efficient catalysts for the Rh-catalyzed enantioselective hydrogenation of a diverse array of substrates (11 examples, from 93% to 99% *ee,* mean *ee* value of 98%).